High-brightness, low-noise, all-fiber photon pair source

Shellee D. Dyer, Burm Baek, and Sae Woo Nam

NIST, Optoelectronics Division, 325 Broadway, Boulder, CO 80305 USA
sdyer@boulder.nist.gov

Abstract: We demonstrate an all-fiber photon pair source for the critical telecom C-band. We achieve high pair generation rates in excess of 10 MHz while maintaining coincidence-to-accidental ratios (CARs) greater than 100. This is one of the brightest and lowest-noise photon pair sources ever demonstrated. We achieve the high pair rate through CW-pumped spontaneous four-wave mixing in dispersion-shifted fiber. We achieve the high CAR by cooling the fiber to 4 K to suppress the Raman generation and detecting the photons with low jitter and low dark count superconducting single-photon detectors.

OCIS codes: (060.4370) Nonlinear optics, fibers; (270.0270) Quantum optics.

References and links

1. J. G. Rarity, J. Fulconis, J. Duligall, W. J. Wadsworth, and P. St. J. Russell, "Photonic crystal fiber source of correlated photon pairs," Opt. Express **13**(2), 534–544 (2005).
2. S. D. Dyer, M. J. Stevens, B. Baek, and S. W. Nam, "High-efficiency, ultra low-noise all-fiber photon-pair source," Opt. Express **16**(13), 9966–9977 (2008).
3. C. Liang, K. F. Lee, M. Medic, P. Kumar, R. H. Hadfield, and S. W. Nam, "Characterization of fiber-generated entangled photon pairs with superconducting single-photon detectors," Opt. Express **15**(3), 1322–1327 (2007).
4. J. B. Altepeter, E. R. Jeffrey, and P. G. Kwiat, "Phase-compensated ultra-bright source of entangled photons," Opt. Express **13**(22), 8951–8959 (2005).
5. F. König, E. J. Mason, F. N. C. Wang, and M. A. Albota, "Efficient and spectrally bright source of polarization-entangled photons," Phys. Rev. A **71**(3), 033805 (2005).
6. Q. Lin, F. Yaman, and G. P. Agrawal, "Photon-pair generation in optical fibers through four-wave mixing: Role of Raman scattering and pump polarization," Phys. Rev. A **75**(2), 023803 (2007).
7. M. J. Stevens, R. H. Hadfield, R. E. Schwall, S. W. Nam, R. P. Mirin, and J. A. Gupta, "Fast lifetime measurements of infrared emitters using a low-jitter superconducting single-photon detector," Appl. Phys. Lett. **89**(3), 031109 (2006).
8. N. R. Newbury, and K. L. Corwin, "Comparison of stimulated and spontaneous scattering measurements of the full wavelength dependence of the Raman gain spectrum," in *Symp. Optical Fiber Measurements*, G W. Day, D. L. Franzen, and P. A. Williams, eds., (NIST Special Publication 988, 2002), p. 7.
9. A. E. Lita, A. J. Miller, and S. W. Nam, "Counting near-infrared single-photons with 95% efficiency," Opt. Express **16**(5), 3032–3040 (2008).
10. K. M. Rosfjord, J. K. W. Yang, E. A. Dauler, A. J. Kerman, V. Anant, B. M. Voronov, G. N. Gol'tsman, and K. K. Berggren, "Nanowire single-photon detector with an integrated optical cavity and anti-reflection coating," Opt. Express **14**(2), 527–534 (2006).

1. Introduction

Fiber-based sources of correlated and entangled photon pairs are attractive because the pairs are generated directly within single-mode fiber, which eliminates the mode-matching losses that can occur when coupling from free-space sources to single-mode fibers. Additionally, fiber-based sources with photon pair generation in the telecommunication C-band are compatible with existing fiber-optic telecom networks for low-loss, single-mode, long-distance transport of the photons. However, fiber-based generation of photon pairs is limited by the strong spontaneous Raman scattering that occurs in fiber. This strong Raman contribution makes it difficult to simultaneously achieve both low-noise and high-brightness

#109788 - $15.00 USD Received 6 Apr 2009; revised 28 May 2009; accepted 30 May 2009; published 4 Jun 2009

operation. In this paper, we use the term noise to describe the unwanted accidental coincidences that are created by Raman photons, multi-pair generation, and detector dark counts, and we use the term brightness to describe photon pair generation rate. Pulsed pumping has typically been used to achieve high pump intensities as well as to reduce the rate of accidental coincidences by reducing the effective time delay window over which coincidences are measured to the narrow time duration of each pulse. However, CW pumping is desirable in order to increase the rate of pair generation. Some previous demonstrations have minimized Raman scattering by choosing a pump wavelength in the normal dispersion regime of the fiber to achieve widely detuned signal and idler photon pairs, which enables CW pumping for high generated pair rates up to 7 MHz without large background photon generation [1]. However, long-distance transmission of those photon pairs is problematic, as they are not single-mode in the standard telecom fiber. In a previous work, we developed a pulsed C-band fiber photon-pair source with coincidence-to-accidental ratio (CAR) of 1300, accomplished by cooling the fiber to 4 K to suppress the Raman scattering [2]. In this paper, we demonstrate a significant increase in the photon-pair generation rate with CW pumping, while maintaining the low-accidental coincidence rate achieved by cooling the fiber to 4 K. The result is the brightest and lowest-noise sources demonstrated to date in the C-band, with a generation rate of more than 10^7 photon pairs per second in a 1 nm filter bandwidth and a coincidence-to-accidental ratio (CAR) of more than 100. This is the first demonstration of a CW-pumped photon pair source with photon pairs in the telecom C-band.

Comparing the brightness of our source with others' results is complicated by the large number of variables that can dramatically affect the source brightness: pair bandwidths, fiber-coupled brightness versus brightness in an iris, generated pair rates versus detected pair rates, pump power, and CAR. Because many authors have used different metrics to quantify source brightness, a side-by-side comparison between our results and others' results is nearly impossible. For example, maximum photon-pair rates for previous demonstrations of fiber-based photon-pair sources in the telecom C-band were around 200 kHz [3], while a free-space spontaneous parametric down-conversion (SPDC) source of entangled photon pairs at a wavelength of 702 nm had photon-pair production rates into 9 mm irises and 25 nm filters exceeding 2 x 10^7 entangled pairs per second [4], but when coupling the output to optical fiber the reported pair rates were much lower, such as 5 x 10^4 /(s·mW) [5]. Often in the literature, photon-pair rates are reported without specifying the corresponding CAR, but we show that it is critical to report both, as photon-pair rates can be increased for any given source by increasing the pump power, but extremely high pump powers yield a lower CAR as a result of multi-pair generation. Both CAR and pair rate are critical parameters in determining source performance.

2. System design

The photon pairs are generated through spontaneous four-wave mixing (FWM) in dispersion-shifted fiber (DSF). The wavelength of the pump laser and the wavelengths of the signal and idler filters must satisfy the phase-matching and energy-matching conditions as follows:

$$k_i + k_s - 2k_p + 2\gamma P_0 = 0\,, \tag{1}$$

and

$$\omega_i + \omega_s - 2\omega_p = 0\,, \tag{2}$$

where k is the propagation constant in the fiber, ω is the radial frequency with subscripts i, s, and p representing the idler, signal and pump, respectively. γ is the fiber nonlinear coefficient, and P_0 is the pump power.

When the pump wavelength is near the zero-dispersion wavelength (ZDW), Eqs. (1) and (2) are satisfied by a broad range of signal and idler wavelength combinations, thus

#109788 - $15.00 USD Received 6 Apr 2009; revised 28 May 2009; accepted 30 May 2009; published 4 Jun 2009

simplifying the phase matching problem [1]. Moreover, we find it helpful to use pump, signal, and idler wavelengths that coincide with the standard ITU (International Telecommunications Union) grid wavelengths, so that we are able to use inexpensive, readily available filters. In our previous work, we found that the zero-dispersion wavelength of our dispersion-shifted fiber is 1549 nm at room temperature and 1544.8 nm at cryogenic temperatures [2]. Here we use a pump wavelength of 1546.1 nm, because it is close to the ZDW and we have the appropriate filters available for this wavelength.

A diagram of our all-fiber photon pair source is shown in Fig. 1. The pump laser is a tunable C-band CW laser diode, which is amplified with an erbium-doped fiber amplifier (EDFA), and then filtered with bandpass filters centered on the pump wavelength to remove the broadband amplified spontaneous emission (ASE) generated by the laser and EDFA. A variable attenuator enables us to characterize the source performance as a function of pump power. The photon pairs are generated by spontaneous FWM in a 300 m length spool of DSF. The signal and idler photons are filtered from the pump photons with a cascaded chain of four 1 nm linewidth bandpass filters centered at the ITU grid wavelengths of 1550.9 nm and 1541.4 nm. In order to minimize the Raman scattering in the conventional single-mode fiber that connects the DSF to the first of the signal filters and to the last of the pump filters, we include pump wavelength filters on either side of the DSF, with fiber pigtails that are as short as possible. In the post-DSF filter we discard the light at the pump wavelength port and use the opposite output port, which transmits both the signal and idler wavelengths with low loss. We measure the photon count rates using superconducting nanowire single-photon detectors (SSPDs) with overall detection efficiencies of 0.8% and 0.4% (this includes the insertion losses of the signal and idler filter chains of approximately 5 dB). The time interval analyzer records a histogram of the relative time delays between clicks recorded on detector 1 and detector 2.

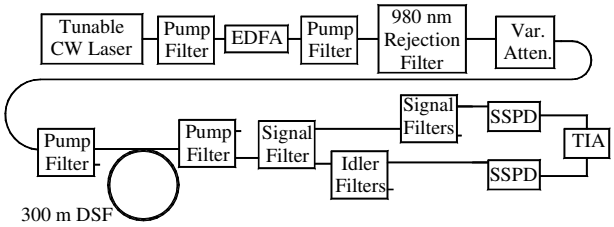

Fig. 1. Simplified diagram of the CW all-fiber photon pair source. DSF = dispersion shifted fiber, TIA = time interval analyzer, SSPD = superconducting nanowire single-photon detector.

Assuming perfect phase matching, the photon pair generation rate can be modeled as

$$I_{pair,u} \approx \left(\gamma P_0 L\right)^2 \int_{-\infty}^{+\infty} \frac{\left|H_u(\omega)\right|^2}{2\pi} d\omega, \tag{3}$$

where the subscript u is either s (signal) or i (idler), γ is the nonlinear coefficient of the fiber, P_0 is the pump power, L is the length of the nonlinear fiber, and $H_u(\omega)$ is the transmission function of the signal or idler filters [6]. Here, we are treating the pump signal as a delta function at the pump frequency. In the case of rectangle function signal and idler filter profiles with identical widths, the integral of Eq. (3) reduces to the filter width $\Delta\nu$, while for the case of Gaussian filters with identical FWHMs of $\Delta\nu$, the integral reduces to $3\Delta\nu/4$. The pair rate predictions of Eq. (3) can also be used for a pulsed pump if we treat P_0 as the peak power, and we multiply Eq. (3) by the duty cycle (D_c) of the pulsed signal.

#109788 - $15.00 USD Received 6 Apr 2009; revised 28 May 2009; accepted 30 May 2009; published 4 Jun 2009

As mentioned above, Raman generation in the fiber contributes a strong noise signal that is added to the photon pair output. Some researchers have reduced the Raman generation by choosing signal and idler wavelengths that are widely detuned (> 15 THz) from the pump wavelength [1], but this would inhibit our goal of developing a source that is suitable for long-distance transmission in standard telecommunications single-mode fiber. Alternatively, we can reduce the Raman scattering by minimizing the frequency detuning between the pump, signal and idler and by cooling the fiber to cryogenic temperatures. The intensity resulting from Raman scattering can be modeled as follows:

$$I_{R,u} \approx \Delta\nu_u P_0 L \left| g_{R,u} \right| \mathrm{N}_u \left(\Omega_s \right), \tag{4}$$

where $I_{R,u}$ is the Raman intensity at the detector (in photons per second), $\Delta\nu_u$ is the bandwidth of the signal and idler filters, L is the fiber length, and $g_{R,u}$ is the Raman gain, which is determined by the properties of the fiber and for small detunings (i.e., less than about 12 THz) increases sharply with the detuning $\Omega_s = \omega_s - \omega_p = \omega_p - \omega_I$ [6]. In contrast with the predictions of Lin et al. [6], we have found that the Raman gain can be measurably different for Stokes versus anti-Stokes scattering; therefore we use the subscript $u = i$ or s to distinguish between Raman scattering at the signal and idler wavelengths. The phonon population is predicted from

$$\mathrm{N}\left(\Omega_s\right) = \begin{cases} \varphi(T, \Omega_s) & \text{for } \omega > \omega_p, \\ \varphi(T, \Omega_s) + 1 & \text{for } \omega < \omega_p, \end{cases} \tag{5}$$

where

$$\varphi(T, \Omega_s) = \left[\exp\left(\frac{\hbar \left| \Omega_s \right|}{k_B T} \right) - 1 \right]^{-1} \tag{6}$$

is the Bose-Einstein temperature-dependent correction factor.

We can use the above equations to predict the coincidence-to-accidental ratio (CAR) of our CW pairs and to compare the CAR to that of a pulsed fiber pair source as follows. For CW pumping, assuming that the photon rates have Poisson probability distributions, then the total number of detected accidental coincidences in an integration time t_{int} is given approximately by

$$N_{acc} \approx t_{\mathrm{int}} t_{win} r_s(t) r_i(t) = t_{\mathrm{int}} t_{win} \left[\eta_i \left(I_{pair} + I_{R,i} \right) + r_{dark} \right] \left[\eta_s \left(I_{pair} + I_{R,s} \right) + r_{dark} \right], \tag{7}$$

where η_i and η_s are the system detection efficiencies of the signal and idler paths (these include the quantum efficiencies of the detector, the losses coupling light from fiber to the detectors, and the insertion losses of the signal and idler filters), r_{dark} is the dark count rate of the detectors, r_s and r_i are the count rates of the signal and idler channels, and t_{win} is the time delay window between the two detectors over which we are looking for coincidences. In Eq. (7) we have assumed that $I_{pair} = I_{pair,s} = I_{pair,i}$, which is valid provided that the signal and idler filters have identical filter profiles. In the system shown in Fig. 1, the true coincidence peak of the measured histogram is broadened around the zero-delay point by the jitter of the SSPDs. This broadening can be modeled as a Gaussian [7], which must be truncated to some finite delay window t_{win} in order to calculate the CAR. The size of t_{win} is important for both pair rate and CAR: if t_{win} is much smaller than the SSPD jitter t_{jitter}, then the measured pair rate will be small because not all of the true coincidences are included within the delay window, but the CAR will be high because few of the accidental coincidences will be recorded within the small t_{win}. Conversely, if t_{win} is much larger than t_{jitter} then we will record most of the true coincidences as well as a large number of the accidental coincidences within t_{win}, yielding a

#109788 - $15.00 USD Received 6 Apr 2009; revised 28 May 2009; accepted 30 May 2009; published 4 Jun 2009

high pair rate but a low CAR. The CAR for CW pumping can be predicted from the accidental and pair rates as follows:

$$CAR_{cw} \approx \frac{\eta_s \eta_i I_{pair} t_{\text{int}} \chi}{N_{acc}}, \tag{8}$$

where χ is the fraction of true coincidences that occur within time delay window t_{win}.

For comparison, the CAR generated by a fiber-based photon pair source with a pulsed pump is given by

$$CAR_{pulsed} \approx \frac{\eta_s \eta_i I_{pair} D_c / f_r}{\left[\eta_s (I_{pair} D_c / f_r + I_{R,s} D_c / f_r) + r_{dark}\right]\left[\eta_i (I_{pair} D_c / f_r + I_{R,i} D_c / f_r) + r_{dark}\right]}, \tag{9}$$

where f_r is the pump repetition frequency. We can then compare the CAR for CW pumping to that of pulsed using Eqs. (7) – (9). If we treat the dark count rate as small compared with the Raman and pair rates, and if we assume that the CW pump power is equal to the peak power of the pulsed case, and that all pairs are detected within the delay window t_{win} (i.e., χ = 1), then we expect that

$$\frac{CAR_{pulsed}}{CAR_{CW}} \approx \frac{t_{win}}{D_c / f_r} \approx \frac{t_{jitter}}{t_{pulse}} \approx \frac{80\,ps}{8\,ps} = 10, \tag{10}$$

where t_{pulse} is the pulse width for the case of a pulsed pump and we have approximated the time delay window t_{win} with the SSPD jitter t_{jitter} of about 80 ps. For comparison to previous work in which we achieved a maximum CAR of 1300 with a pulsed pump, we assume a pulse width of 8 ps, which corresponds to a 1 nm linewidth for the pulses [2]. From this we expect a maximum CAR for our CW pumping experiments of around 130. However, the CAR results that we report in this paper are higher because we have improved the pump filtering in our system compared to that used in our previous pulsed measurements [2].

3. Measurement results

3.1 Raman characterization

In order to compare our measurement results with the predicted CAR of Eq. (8), it is necessary to know reasonable values for the fiber parameters, such as Raman gain and nonlinear coefficient. For the nonlinear coefficient, we use 2.2 $W^{-1} \bullet km^{-1}$, as obtained from our prior work [2]. For the Raman gain, we found that our previous Raman gain characterization was skewed slightly by pump photon leakage, therefore we show a new Raman characterization measurement here. We have since added additional filters to further reduce pump photon leakage. Also, we have improved our Raman characterization with a new measurement based on the work of Newbury et al. [8], which is shown in Fig. 2. In this system we use a double-grating optical spectrum analyzer (OSA) to measure the Raman spectrum from 300 m of dispersion-shifted fiber. We repeated this measurement for the cases where the nonlinear fiber was held at room temperature, 77 K, and 4 K, and we found that this measurement works best at room temperature, because at lower temperatures the Raman spectrum is so weak that it approaches the noise floor of the OSA. We measure the backscattered spectrum, because we expect the Raman scattering to be isotropic, and we expect that the photon pairs will propagate only in the forward direction. From the measured spectra and Eq. (4), we can calculate the Raman gain spectrum, as shown in Fig. 3(a). To be consistent with others' work, we have separated the Raman gain spectrum into the Stokes and anti-Stokes components and plotted the results as a function of frequency detuning. From this figure, we see that for small detunings there is little difference between the Stokes and anti-Stokes Raman gains; however, for large detunings, the difference is significant. In Fig. 3(b)

#109788 - $15.00 USD Received 6 Apr 2009; revised 28 May 2009; accepted 30 May 2009; published 4 Jun 2009

we show the Raman photon generation rates (normalized to 1 mW of pump power) calculated from the data of Fig. 3(a). We show results for both T = 300 K and T = 4 K, but we have omitted the anti-Stokes curve at 4 K because it is so small. From these results, it is clear that the Raman scattering can be minimized by either making the detuning as small as possible or by going to a very large detuning (> 15 THz). For this work, we used a small detuning of 0.6 THz; from Fig. 3(a) we find that the Raman gains for this detuning are $g_{R,S} = 0.04\ \mathrm{W}^{-1} \bullet \mathrm{km}^{-1}$ and $g_{R,aS} = 0.03\ \mathrm{W}^{-1} \bullet \mathrm{km}^{-1}$.

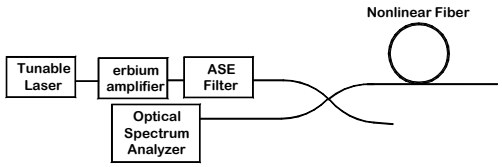

Fig. 2. System used to characterize the Raman gain by measuring the backscattered spectrum.

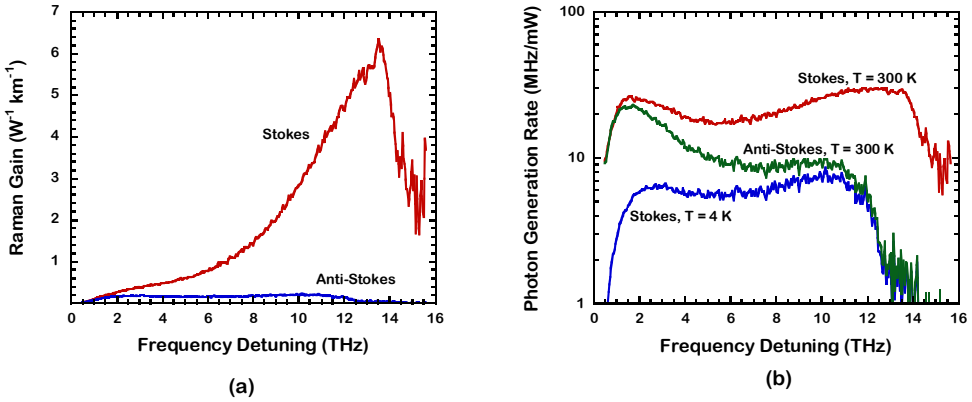

Fig. 3. (a). Measured Raman gain spectra as a function of the detuning between the signal and pump frequencies. (b). Plot of the Raman photon generation rates (normalized to 1 mW of CW pump power), calculated from the measured Raman gain data of (a) for T = 300 K and T = 4 K. The anti-Stokes Raman at 4 K is not shown because it is too small to be plotted here.

3.2 CAR measurement results

The TIA analyzer shown in Fig. 1 records a histogram of the relative time delays between clicks recorded on detector 1 and detector 2. In the absence of detector and electronic jitter, the true coincidence counts, which occur when the two detectors each click on one-half of a single pair, would occur exactly at the zero delay point of the histogram. However, the jitter of the SSPDs (approximately 80 ps) broadens the zero-delay coincidence peak; therefore we fit a Gaussian to the histogram with the peak, width, and DC value as free parameters. We calculate the total true coincidence counts by subtracting the DC value, truncating the Gaussian to some finite time-delay width, and integrating the number of counts in the Gaussian within that truncated delay width. The average number of accidental coincidence counts per bin is approximately equal to the DC value of the curve fit, and we estimate the total number of accidental coincidences from the product of that DC value with the same truncated delay width that we used to calculate the true coincidences. We can then determine the CAR as the ratio of the total number of true coincidences to the total number of accidental coincidences, where both are calculated within the same delay width. Choosing the time delay width for the integration is a tradeoff between CAR and pair rate: a wider delay integration

#109788 - $15.00 USD Received 6 Apr 2009; revised 28 May 2009; accepted 30 May 2009; published 4 Jun 2009

width will include more coincidence counts and yield a higher pair rate, but it also includes more of the accidental coincidences, resulting in a lower CAR. Conversely, the highest possible CAR occurs when the integration width is infinitesimally small, and is equal to the histogram's peak value divided by the DC value, but in this case the rate of pairs in that integration area approaches zero. As a compromise between high CAR and high pair rate, we decided to integrate over a time delay equal to the 1/e full-width of the true coincidence peak; this time delay maximizes the product of the CAR and the pair rate. We also estimate the pair rate by dividing our true coincidence count estimate by the integration time of the histogram. We distinguish between *detected* pair rate and *generated* pair rate, where the two are related by the product of the system detection efficiencies (DE) of the two detector channels. We define the system DE as the product of the detector quantum efficiency with any coupling losses from fiber to detector and with the total losses of the signal and idler filter chains, for total DEs of 0.008 (signal arm) and 0.004 (idler arm).

In Fig. 4(a) we show measured and predicted values for CAR (left hand axis) versus pump power and for generated pair rate (right hand axis) versus pump power. The predictions are calculated from Eq. (8) for CAR and Eq. (3) for pair rate. The measured CARs were calculated from the measured histogram data as described above, where the integration time of each histogram was chosen based on the pump power so that each histogram had approximately the same number of coincidences regardless of pump power. For example, the lowest pump power for which we collected a histogram was 1 mW, while the highest pump power was 32 mW, and we integrated these histograms for 256 and 0.25 s, respectively. The CAR is reduced at higher pump powers because the pair rate increases quadratically with pump power, yielding an increased probability of detecting multiple pairs within a given time window. For comparison, at low pump powers the dark count rate of the detectors (typically 100 Hz) becomes significant and the CAR decreases. Thus an optimal pump power must be chosen with consideration of both high CAR and high pair rate. This tradeoff is illustrated in Fig. 4(b) where we plot the CAR versus generated pair rates.

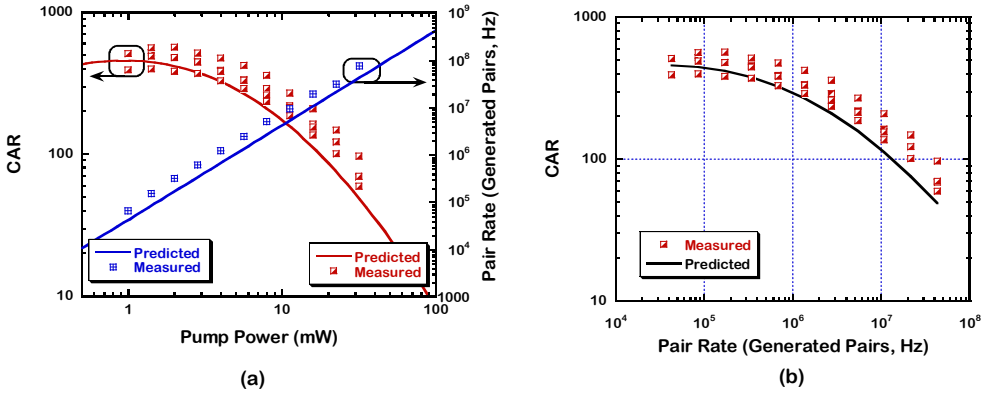

Fig. 4. (a). Plot of CAR versus pump power (left axis) and generated pair rate versus pump power (right axis). These are the photon pair rates generated within the 1 nm linewidth of the signal and idler filters. CAR data are shown from 4 repeated measurements. (b). Plot showing the tradeoff between high CAR and high pair rates.

4. Discussion

Although the detected pair rate could be increased significantly if we were to replace the SSPDs with transition-edge sensor (TES) single-photon detectors with quantum efficiencies of 95% [9], in that case the CAR would be unacceptably low, because the TES jitter is approximately 1000 times larger than that of the SSPD. A better option for increasing the

#109788 - $15.00 USD Received 6 Apr 2009; revised 28 May 2009; accepted 30 May 2009; published 4 Jun 2009

detected pair rates would be to use the new high quantum efficiency SSPDs, with reported quantum efficiencies around 50% [10].

5. Conclusions

We have demonstrated an all-fiber, CW pumped source with the highest rate of photon pair generation and lowest noise ever demonstrated in the critical telecom C-band. We have shown that we can achieve generated pair rates as high as 10^7 Hz while simultaneously demonstrating a CAR greater than 100. Another key point about this source is that we are able to generate photon pairs at rates higher than 10 MHz with a CW pump power less than 20 mW. Therefore, it should be possible to apply this source to quantum repeater applications such as entanglement swapping and teleportation without the need for expensive pump lasers and EDFAs.

#109788 - $15.00 USD Received 6 Apr 2009; revised 28 May 2009; accepted 30 May 2009; published 4 Jun 2009